Quantitative analysis of breast parenchymal patterns using 3D fibroglandular tissues segmented based on MRI

Ke Nie and Daniel Chang
Tu and Yuen Center for Functional Onco-Imaging, University of California, Irvine, California 92697

Jeon-Hor Chen
Tu and Yuen Center for Functional Onco-Imaging, University of California, Irvine, California 92697 and Department of Radiology, China Medical University Hospital, Taichung 404, Taiwan

Chieh-Chih Hsu
Department of Radiology, China Medical University Hospital, Taichung 404, Taiwan

Orhan Nalcioglu and Min-Ying Su[a)]
Tu and Yuen Center for Functional Onco-Imaging, University of California, Irvine, California 92697

(Received 21 May 2009; revised 24 October 2009; accepted for publication 10 November 2009; published 9 December 2009)

Purpose: Mammographic density and breast parenchymal patterns (the relative distribution of fatty and fibroglandular tissue) have been shown to be associated with the risk of developing breast cancer. Percent breast density as determined by mammography is a well-established risk factor, but on the other hand, studies on parenchymal pattern have been scarce, possibly due to the lack of reliable quantitative parameters that can be used to analyze parenchymal tissue distribution. In this study the morphology of fibroglandular tissue distribution was analyzed using three-dimensional breast MRI, which is not subject to the tissue overlapping problem.
Methods: Four parameters, circularity, convexity, irregularity, and compactness, which are sensitive to the shape and margin of segmented fibroglandular tissue, were analyzed for 230 patients. Cases were assigned to one of two distinct parenchymal breast patterns: Intermingled pattern with intermixed fatty and fibroglandular tissue (Type I, $N=141$), and central pattern with confined fibroglandular tissue inside surrounded by fatty tissue outside (Type C, $N=89$). For each analyzed parameter, the differentiation between these two patterns was analyzed using a two-tailed t-test based on transformed parameters to normal distribution, as well as distribution histograms and ROC analysis.
Results: These two groups of patients were well matched both in age (50 ± 11 vs 50 ± 11) and in fibroglandular tissue volume (Type I: 104 ± 62 cm^3 vs Type C: 112 ± 73 cm^3). Between Type I and Type C breasts, all four morphological parameters showed significant differences that could be used to differentiate between the two breast types. In the ROC analysis, among all four parameters, the "compactness" could achieve the highest area under the curve of 0.84, and when all four parameters were combined, the AUC could be further increased to 0.94.
Conclusions: The results suggest that these morphological parameters analyzed from 3D MRI can be used to distinguish between intermingled and central dense tissue distribution patterns, and hence may be used to characterize breast parenchymal pattern quantitatively. The availability of these quantitative morphological parameters may facilitate the investigation of the relationship between parenchymal pattern and breast cancer risk. [DOI: 10.1118/1.3271346]

Key words: three-dimensional MRI, 3D breast parenchymal morphology, quantitative breast density

I. INTRODUCTION

Mammary gland architecture may play an important role in determining the susceptibility of developing breast cancer.[1,2] The most well-studied parameter is mammographic density, evaluated as the percentage of dense tissue area over the total breast area on mammograms. There are numerous studies reporting mammographic density as a strong risk factor; the higher the percentage, the higher the breast cancer risk.[3–8] Increased density over time has also been shown to be associated with higher cancer incidence.[9–11] There is also evidence suggesting that the relative distribution of adipose and fibroglandular tissue (referred as the breast parenchymal pattern in this work) is involved in cancer development. The adipose tissue that is abundantly present around the ductal epithelium of the mammary gland may function as a slow release depot for lipid-soluble carcinogenic agents, and thus may affect cancer risk.[12,13] However, the relationship between parenchymal pattern and cancer risk has never been

reported, possibly due to the lack of both the imaging modality necessary to reveal the distribution pattern and the appropriate analysis methods.

Several studies have applied texture analysis to analyze the distribution pattern of the projected dense tissue on mammograms,[1,14,15] and shown differences between women with invasive cancer and women without cancer.[15] There are also differences between high-risk women carrying the BRCA1 and BRCA2 gene and low-risk women,[1,14] which is possibly due to lobular branching promoted by these genes.[2] Since the mammogram is a two-dimensional (2D) projection image, texture analysis can be used to characterize the amount and/or the heterogeneity/homogeneity of dense tissue. However, as these features arise in part from the way that tissues overlap on the projected image, the analyzed parameters may be affected by different positioning of the breast and the degrees of compression. A three-dimensional (3D) imaging technique is needed to reveal the respective distribution of the fatty and fibroglandular tissues. The investigation of the relationship between cancer risk and breast parenchymal pattern will only be meaningful when the parameters can be reliably measured.

MRI provides 3D images of the breast, and that allows for the slice-by-slice segmentation of the fibroglandular and the fatty tissues for the evaluation of breast parenchymal pattern. To date, only a few studies have investigated the percent breast density using MRI, and the relative distribution pattern of the fatty and fibroglandular tissues has not yet been reported. The wealth of the 3D information that can be provided by MRI has yet to be fully explored. With the establishment of the American Cancer Society guidelines for annual MRI screening for high-risk women, many more clinical breast MRI examinations will be performed. Development of reliable methods to measure the extent of density and to characterize the parenchymal pattern may provide additional information contributing to a better management plan for these women.

We have published an analysis method utilizing computer algorithms to segment the fibroglandular tissue for quantitative measurement of the percent density in the whole breast using MRI.[16] In the present study we hope to address a new question: In addition to the percent density, can we use quantitative parameters to characterize the distribution pattern of the dense tissues? As an initial approach, we analyzed two distinct breast parenchymal patterns that can be classified visually: The intermingled pattern with intermixed fatty and fibroglandular tissues, and the central pattern with confined fibroglandular tissue inside surrounded by fatty tissue outside. Breasts from these two groups may have comparable percent densities but differ in the distribution pattern of their dense tissue. Four different morphological parameters were calculated based on the 3D distribution pattern of segmented fibroglandular tissues, and their capacity to differentiate between the intermingled and the central patterns were evaluated using respective histograms and the receiver operating characteristic (ROC) analysis.

In medical imaging, the ROC analysis is commonly used for differentiating between malignant and benign tumors, with "sensitivity" as the ability to correctly diagnose malignant lesions and "specificity" as the ability to correctly diagnose benign lesions. In this work, the ROC analysis is used to differentiate between two different breast parenchymal patterns shown on MRI, the central pattern (Type C) and the intermingled pattern (Type I), using the radiologist's reading as the ground truth; sensitivity referred to the ability to correctly diagnose Type I, and specificity referred to the ability to correctly diagnose Type C. In order to better understand the physical representation of the analyzed morphological parameters, cases with high and low index parameters were graphically depicted for visual comparison. The parameter that can differentiate between these two distinct patterns may then be used to provide a quantitative measure of parenchymal patterns, to facilitate the investigation of the relationship between parenchymal pattern and cancer risk.

II. MATERIALS AND METHODS

II.A. Patient database

In a review of our IRB-approved research breast MRI database from 2004 to 2006, 509 consecutive patients with either suspicious lesions or confirmed breast cancer were studied. Of these, 301 patients who had unilateral breast disease and for whom age and race information was available were included in this study. The radiology and pathology reports for each patient were reviewed to confirm that the disease was present in only one breast, and the breast density was only analyzed for the normal contralateral breast. Patients who had fatty breasts with the percent density $<7\%$ ($N=71$) as measured by MRI were classified as the fatty breast group. An example is shown in Fig. 1(a). Since this group could easily be classified based on percent density alone, they were not included in morphology analysis. The remaining 230 patients were used for the analysis of breast parenchymal pattern.

The MRI studies were acquired using a Philips Eclipse 1.5T scanner. The images were acquired using a nonfat sat T1-weighted 3D SPGR (RF-FAST) pulse sequence, with TR=8.1 ms, TE=4.0 ms, flip angle=20°, matrix size=256 $\times$256, and field of view varying between 32 and 38 cm. A fixed number of 32 slices, each 4 mm thick, were used to cover the whole breasts. All 32 imaging slices were analyzed.

II.B. Classification of breast parenchymal pattern to Type I vs Type C

The parenchymal pattern of each case was classified into one of two types that are commonly seen on breast MRI: Type I, the intermingled pattern with mixed fatty and fibroglandular tissues, and Type C, the central pattern with confined fibroglandular tissue inside surrounded by fat outside. The criteria used to differentiate between the two patterns were as follows: The central pattern was assigned when (1) most of the fibroglandular tissue was centrally located and peripherally surrounded by fatty tissue, (2) the interface between fatty and dense tissues could either be smooth or ir-

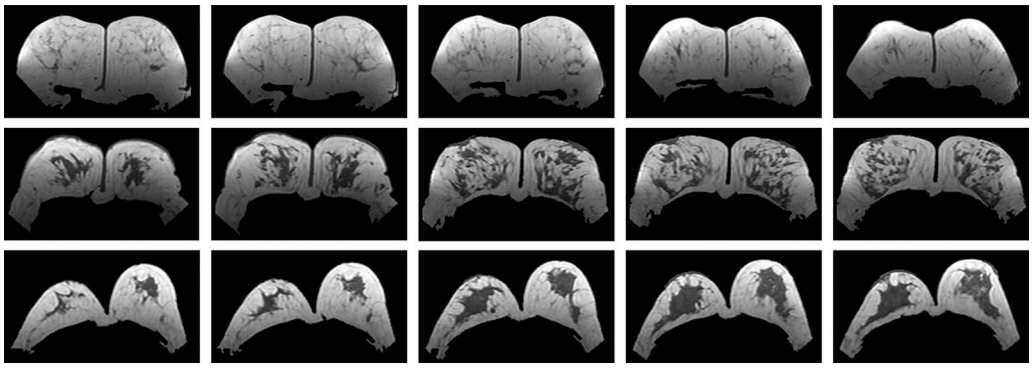

FIG. 1. Three case examples are demonstrated, including one fatty breast (top row), one Type I case (intermingled pattern, middle row), and one Type C case (central pattern, bottom row). For each case, five axial view MR images from five imaging slices selected from superior to inferior directions are shown. There are no breast lesions on these images. The percent density is 5.4% for the fatty breast, 14.1% for the Type I case, and 13.9% for the Type C case.

regular, and (3) a small amount of scattered fatty tissues could be present within the fibroglandular tissue. If the criteria for the central pattern were not met, the case was assigned to the intermingled pattern group. For extreme cases of the intermingled pattern, the fibroglandular and fatty tissues could be intermixed throughout the entire breast.

The parenchymal patterns of all cases were visually inspected twice by an experienced radiologist (J. H. Chen) and once by an experienced physicist (K. Nie) using the same criteria. They were blind to each other's assignments. Between the first and second reading of the radiologist, there were eight discrepant cases among 230 cases (3.5%). There were six discrepant cases (2.6%) between the physicist's reading and radiologist's first reading, and 14 discrepant cases (6%) between physicist's reading and radiologist's second reading. All discrepant cases were reviewed by both observers together to reach a consensus agreement, and this consensus assignment was used as the ground truth. Finally, of the 230 cases, $N=141$ was classified as Type I, and $N=89$ was classified as Type C. Figure 1(b) shows a typical intermingled pattern (Type I), with mixed fibroglandular tissues and fatty tissues throughout the whole breast. Figure 1(c) illustrates a typical example of Type C, showing confined fibroglandular tissue inside surrounded by fatty tissue outside.

II.C. Quantitative assessment of breast parenchymal patterns

The whole breast and the fibroglandular tissues were segmented on each slice using a computerized method developed by our group.[16] An initial cut of the breast region based on each individual woman's body landmarks was performed, and then the boundary of the breast was determined using clustering-based segmentation with the *b*-spline curve fitting to exclude chest wall muscle, followed by dynamic searching to exclude skin. Then, within the segmented breast, the adaptive fuzzy c-means clustering algorithm was applied to segment the fibroglandular tissues.

Based on the segmentation results from all 32 slices, the total fibroglandular tissue volume and the percent density normalized to total breast volume were calculated. Figure 2 shows the bar plot of the age, fibroglandular tissue volume, and the percent density of the three subject groups for comparison, which consist of fatty ($N=71$), Type I ($N=141$), and Type C ($N=89$) breasts. It can be seen that the fatty breast group is significantly older, and this group can be well separated from the other two groups based on the lower dense tissue volume or the lower percent density. However, breasts from the Type I and Type C groups have comparable age, dense tissue volume, and percent density, and thus cannot be separated.

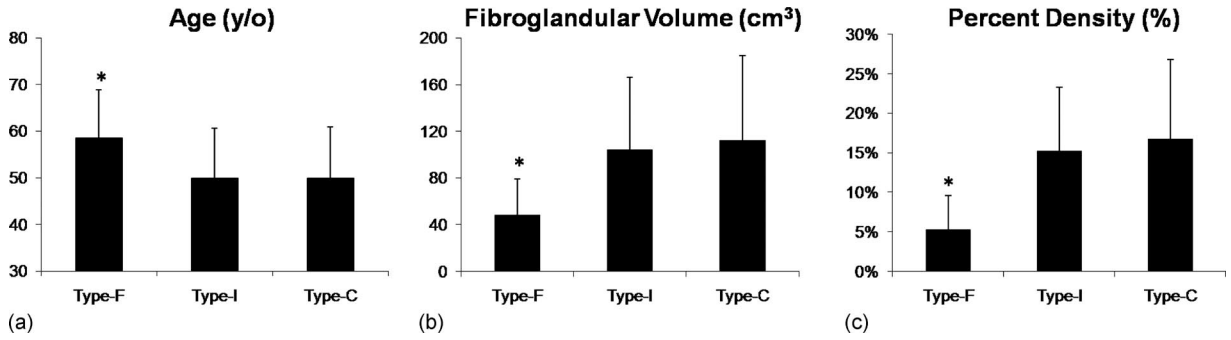

FIG. 2. The bar plot for comparing the (a) age, (b) fibroglandular tissue volume, and (c) the percent density among three subject groups. The fatty breast group (indicated as Type F) is significantly older, and has the smallest fibroglandular tissue volume and the lowest percent density compared to the intermingled type (Type I) and the central type (Type C). The Type I and Type C groups have comparable age, fibroglandular tissue volume, and the percent density, thus they cannot be separated based on these parameters.

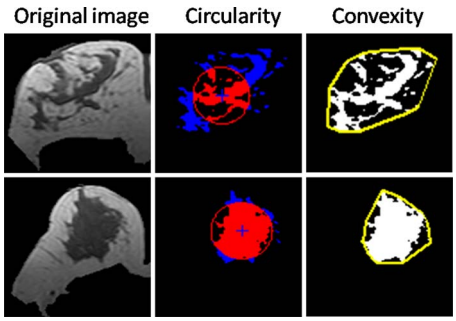

FIG. 3. Illustration of the calculation of the circularity and the convexity index. Only one slice is shown here as an example, but the analysis was performed in 3D. For circularity, a sphere with effective diameter D_{eff} is drawn, and the ratio between the fibroglandular tissue volume within the sphere and the total fibroglandular tissue volume is calculated as the circularity index. The intermingled pattern (top) has a circularity index of 0.42 and the central pattern (bottom) has a higher index of 0.86. For convexity, the minimum convex hull is drawn, and the ratio between the total fibroglandular tissue volume and the convex hall volume is calculated as the convexity index. The intermingled pattern (top) has a convexity index of 0.36 and the central pattern (bottom) has a higher index of 0.73.

In order to characterize the different morphological distribution patterns between Type I and Type C, we analyzed four morphological parameters that are sensitive to shape ("circularity" and "convexity") and margin (related to the ratio between the surface area and the total volume, "irregularity" and "compactness") for the segmented fibroglandular tissues.

(1) Circularity defined as

$$\text{Circularity} = \frac{V_{\text{within}}}{V_{\text{fibro}}},$$

where V_{within} is the volume of fibroglandular tissue within the sphere of effective diameter $D_{\text{eff}} = 2 \times \sqrt[3]{3 \cdot V_{\text{fibro}}/4}$, and V_{fibro} is the total volume of fibroglandular tissue, as illustrated in Fig. 3. The centroid of the fibroglandular tissues was first identified, and a sphere with diameter of D_{eff} was drawn. The volume of the fibroglandular tissues within the sphere was measured, and the ratio to the total fibroglandular tissue was defined as the circularity. As shown in Fig. 3, the case with the central pattern has the V_{within} close to the V_{fibro} and hence has a higher circularity compared to the case with the intermingled pattern. A perfect sphere will have the highest circularity index of one.

(2) Convexity defined as

$$\text{Convexity} = \frac{V_{\text{fibro}}}{V_{\text{convex}}},$$

where V_{convex} is the volume of the minimum convex hull containing the border voxels identified using the gift wrapping algorithm,[17] as illustrated in Fig. 3. The gift wrapping algorithm is performed as follows: Starting from the leftmost vertex, at each step the polygon formed by three consecutive vertices is inspected. If the resulting angle is concave, then the middle point is discarded and the next vertex (along the polygon) is added for testing. If the angle is convex, then the process is repeated by moving to the next vertex. As shown in Fig. 3, the case with the central pattern has the convex volume closer to the fibroglandular tissue volume, and hence has a higher convexity index compared to the case with the intermingled pattern. A perfect sphere will have the highest convexity index of 1.

(3) Irregularity defined as

$$\text{Irregularity} = 1 - \frac{\pi \cdot D_{\text{eff}}^2}{S_{\text{fibro}}},$$

where S_{fibro} is the surface area of fibroglandular tissue. The irregularity index compares the total surface area to the surface area of a sphere with effective diameter D_{eff}. A perfect sphere will have the lowest irregularity index of zero.

(4) Compactness defined as

$$\text{Compactness} = \frac{S_{\text{fibro}}^{3/2}}{V_{\text{fibro}}}.$$

The compactness is related to the ratio between the total surface area and the total volume. A sphere with smooth boundaries will have the lowest compactness index. A highly nonconvex pattern with rough boundaries will have a high compactness index.

II.D. Statistical analysis

The distributions of each analyzed parameter in all patients were examined using the Kolmogorov–Smirnov test, and were transformed to normal distribution for statistical analysis. The parameters of "age" and circularity were already normally distributed, and did not need further transformation. The natural logarithm (ln) transformation was applied to fibroglandular tissue volume, while the square root (sqrt) transformation was applied to the parameters "percent density," convexity, irregularity, and compactness.

Two-way analysis of variance was used to examine mean differences among the three parenchymal patterns of fatty, intermingled (Type I), and central (Type C) for age, (ln) fibroglandular tissue volume, and (sqrt) percent density. The ability of the four morphological parameters (circularity, convexity, irregularity, and compactness) to differentiate between the intermingled (Type I) and the central pattern (Type C) groups was first evaluated using a two-tailed *t*-test for the transformed parameters. For each morphological parameter, the values from all analyzed cases were ranked in order, and the distribution between the Type I and Type C patterns was plotted as histograms for comparison. Two cases with comparable densities, one with high index and one with low index (selected from the neighborhood of #35 and #195 ranking among all 230 cases), were graphically depicted as examples for visual inspection of their different parenchymal distribution patterns.

In addition to the individual analysis of each parameter, the linear regression model (enter method) using all four pa-

TABLE I. Comparison of age, fibroglandular tissue volume, percent density, and morphological parameters between two groups with intermingled pattern and central pattern.

	Type I, intermingled pattern ($N=141$)	Type C, central pattern ($N=89$)	t-test[a] P value
Age (years old)	50 ± 11	50 ± 11	NS
Fibroglandular volume (cm^3)	104 ± 62	112 ± 73	NS
Percent density (%)	15.3 ± 8.1	16.7 ± 10.1	NS
Circularity index	0.36 ± 0.13	0.50 ± 0.12	$p<0.001$
Convexity index	0.27 ± 0.08	0.38 ± 0.10	$p<0.001$
Irregularity index	0.69 ± 0.07	0.61 ± 0.09	$p<0.001$
Compactness index	14.2 ± 5.2	8.6 ± 4.5	$p<0.001$

[a]t-test was performed based on transformed parameters to normal distribution. Age and Circularity were normally distributed. The ln was applied to transform the fibroglandular tissue volume and the sqrt was applied to transform the other four parameters.

rameters together was applied to evaluate differences between the Type I and Type C patterns. The performance was evaluated using the ROC analysis with fourfold cross-validation. All cases were first randomly assigned into four subcohorts, with each subcohort containing approximately the same proportion of Type C and Type I cases. Three subcohorts were combined as the training set and the remaining subcohort was used as the validating set. For each training set, logistic model selection was applied to all four morphological features. The generated models were then applied to its corresponding validating set. Then, the determined diagnostic classifier could be used to predict a parenchymal pattern being Type I or Type C, based on the threshold level. The sensitivity was defined as the ability to correctly classify the intermingled pattern (Type I), while specificity was defined as the ability to correctly classify the central type (Type C). The sensitivity and specificity in the entire data set were calculated from a full range of thresholds (from 0.0–1.0 with an interval of 0.05), and then the ROC curve was constructed using all data points at different thresholds by plotting sensitivity vs one specificity. The area under the ROC curve (AUC) of all models were then listed in ascending order, and the one with the highest AUC was chosen. Finally, this model was applied to the entire cohort to obtain the final classification results. All analyses were performed using the SPSS 15.0 package (SPSS Inc., Chicago, IL).

III. RESULTS

III.A. Age, fibroglandular tissue volume, and percent density

As shown in Fig. 2, the fatty breast group could be easily separated from the Type I and Type C groups. They were significantly older in age (59 ± 10 yr old), and had significantly lower fibroglandular tissue volume (48 ± 31 cm^3) and lower percent density ($5.2 \pm 4.4\%$). The mean age of patients was 50 ± 11 yr old in the intermingled pattern (Type I) group and 50 ± 11 yr old in the central pattern (Type C) group, so these two groups were well matched in age. The mean fibroglandular tissue volumes in these two groups were (Type I: 104 ± 62 cm^3 vs Type C: 112 ± 73 cm^3), and the percent densities were (Type I: $15.3 \pm 8.1\%$ vs Type C: $16.7 \pm 10.1\%$). The density was slightly higher in the central pattern group, but the difference was not statistically significant.

III.B. Morphological parameters

The results of all density parameters calculated from the segmented fibroglandular tissues for Type I (intermingled) and Type C (central) cases are summarized in Table I. The four morphological parameters circularity, convexity, irregularity, and compactness all showed significant differences between the two patterns when comparing the transformed parameters (to the normal distribution) using the two-tailed t-test, suggesting that these features may be used to quantitatively characterize the parenchymal patterns. Figure 4 shows the relative distribution histograms of these four morphological features between Type I (intermingled) and Type C (central) groups. Different distribution curves in these two patterns were clearly noted. In order to better understand the link between these quantitative parameters and the physical representation of fibroglandular tissue distributions, the indices from all 230 cases were sorted in ascending order, and the cases with comparable percent density but with high ranking (#180–210/230) vs low ranking (#20–50/230) indices were selected for visual comparison.

III.B.1. Morphological feature—circularity

Two examples are demonstrated in Fig. 5 to illustrate the circularity index, which is defined to analyze the shape of the distribution relative to a sphere of effective diameter. The two cases have similar percent densities (9.6% vs 9.8%) but different parenchymal distribution patterns. Figure 5(a) shows a linearly structured fibroglandular pattern with a low circularity index=0.29 (ranking #33/230, Type I), and the Fig. 5(b) case shows a round fibroglandular region with a high circularity index=0.58 (ranking #187/230, Type C). In all 230 cases, the circularity index was significantly lower for the intermingled pattern than for the central pattern (0.36 ± 0.13 vs 0.50 ± 0.12, $p<0.001$).

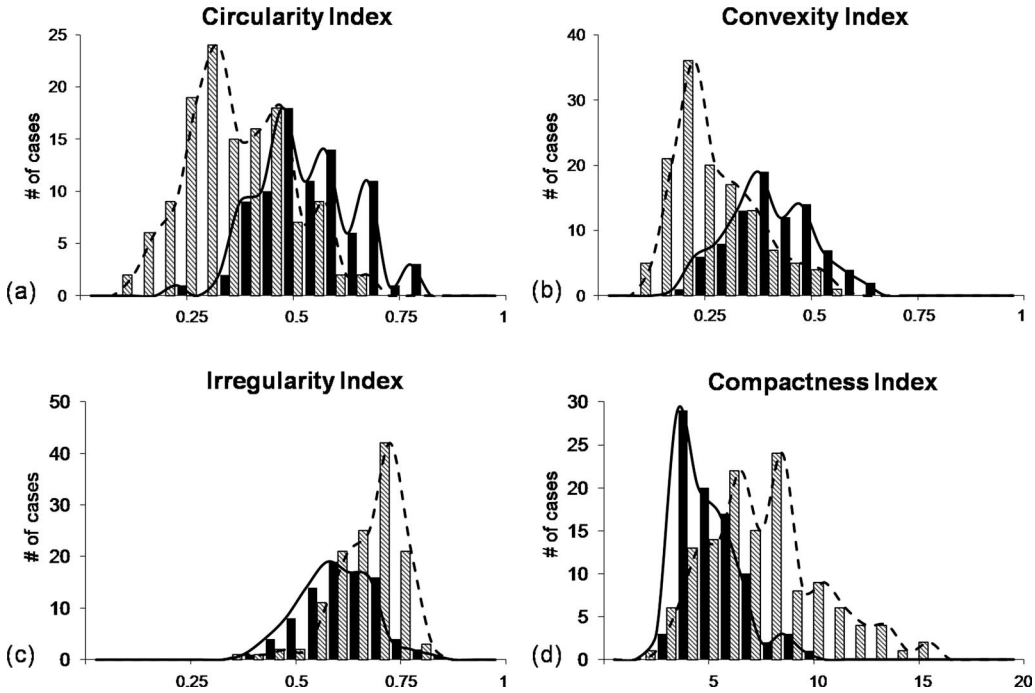

FIG. 4. Histogram of four morphological parameters differentiating the intermingled pattern (Type I, dashed curve) and the central pattern (Type C, solid curve), (a) circularity index, (b) convexity index, (c) irregularity index, and (d) compactness index. The intermingled pattern group has lower circularity and convexity, and higher irregularity and compactness compared to the central pattern group. The cases with high and low indices are illustrated in Figs. 5–8.

III.B.2. Morphological feature—convexity

The convexity index is defined to analyze the shape with respect to the minimum convex hull containing the border voxels. Two examples are demonstrated in Fig. 6. The top case, with a low convexity index=0.20 (ranking #30/230, Type I), has a lower occupancy within the corresponding convex hulled area, while the bottom case, with a high convexity index=0.46 (ranking #180/230, Type C), has a higher occupancy. These two cases have comparable percent densities (10.9% vs 11.6%). In all 230 cases, the convexity index was significantly lower for the intermingled pattern than for the central pattern (0.27 ± 0.08 vs 0.38 ± 0.10, $p < 0.001$).

III.B.3. Morphological feature—irregularity

The irregularity index is defined to compare the total surface area to the surface area of a sphere with effective diameter D_{eff}. Two examples with high and low irregularity indices are shown on Fig. 7. They have similar percent densities (15.1% vs 15.6%) but different parenchymal distribution patterns. The case with a high irregularity index=0.74 (ranking

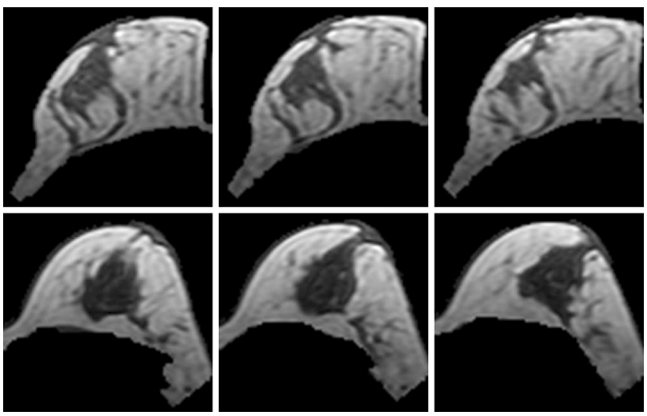

FIG. 5. The circularity index is sensitive to the spherical vs nonspherical shapes. The top case is an intermingled pattern with percent density =9.6% and circularity index=0.29, ranking 33 in all 230 cases. The bottom case is a central pattern with a similar percent density=9.8%, and a higher circularity index=0.58, ranking 187 in all 230 cases.

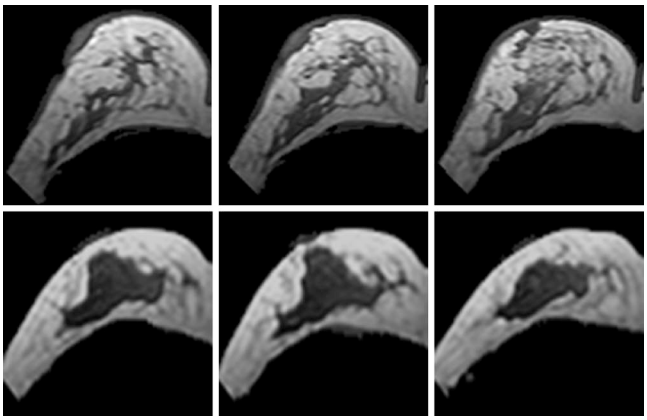

FIG. 6. The convexity index is sensitive to the convex vs concave shapes. The top case is an intermingled pattern with percent density=10.9% and convexity index=0.20, ranking #30 in all 230 cases. The bottom case is a central pattern with percent density=11.6%, and a higher convexity index =0.46, ranking #180 in all 230 cases.

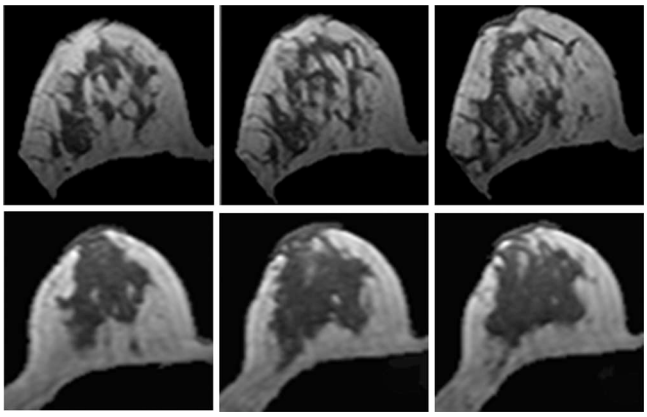

FIG. 7. The irregularity index is sensitive to the irregular vs smooth margins. The top case is an intermingled pattern with percent density=15.1% and irregularity index=0.74, ranking #190 in all 230 cases. The bottom case is a central pattern with percent density=15.6%, and a lower irregularity index=0.54, ranking #26 in all 230 cases.

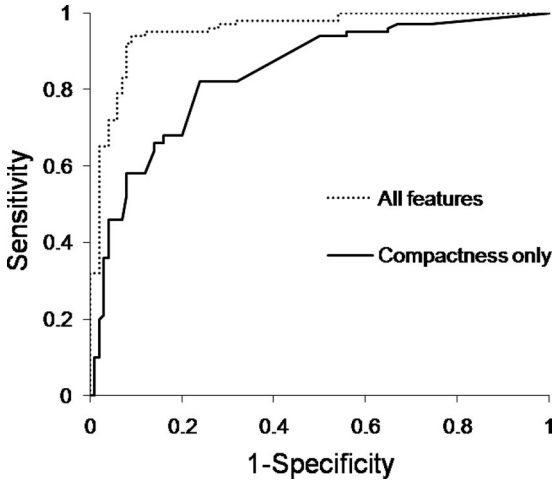

FIG. 9. The ROC curves. When only using the compactness index the AUC is 0.84, and when using all four morphology parameters combined, the AUC is improved to 0.94.

#190/230) has an intermingled pattern showing an irregular border, and the case with a low irregularity index=0.54 (ranking #26/230) has a central pattern with a smooth border. In all 230 cases, the irregularity index was significantly higher for the intermingled pattern compared to the central pattern (0.69 ± 0.07 vs 0.61 ± 0.09, $p < 0.001$).

III.B.4. Morphological feature—compactness

The compactness index is defined to compare the ratio between the total surface area and the total volume. Two cases with comparable percent densities (Type I: 12.9% vs Type C: 11.8%) are shown in Fig. 8. The case with a high compactness index=17.5 (ranking #180/230) has an intermingled pattern, and the case with a low index=6.7 (ranking #32/230) has a central pattern. In all 230 cases, the compactness index was higher for the intermingled pattern than for the central pattern (14.2 ± 5.2 vs 8.6 ± 4.5, $p < 0.001$). Among all four analyzed morphological parameters, the compactness index was the best parameter to differentiate between these two parenchymal patterns, and showed the widest separation between the histogram curves of these two groups, as shown in Fig. 4(d).

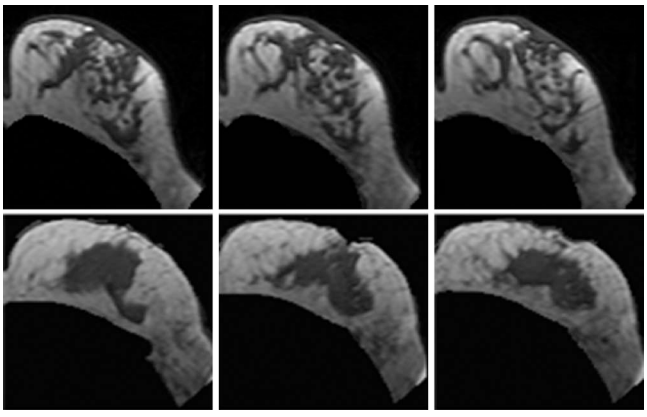

FIG. 8. The compactness index is sensitive to both shape and margin. Round shape with smooth margin has a relatively low compactness index. The top case is an intermingled pattern with percent density=12.9% and compactness index=17.5, ranking #180 in all 230 cases. The bottom case is a central pattern with the percent density=11.8%, and a lower compactness index =6.7, ranking #32 in all 230 cases.

III.C. Group differentiation using ROC analysis

The power of these four morphological parameters in differentiating between the Type I and Type C patterns was analyzed individually using ROC analysis. As suggested by the histogram analysis shown in Fig. 4, the compactness index was the best single predictor among all four parameters, which attained the highest AUC of 0.84. These four parameters have distinctly different definitions, and in theory, they are sensitive to different aspects of the distribution. However, in reality, they are all related to shape and margin, and are highly correlated. When all four morphological parameters were combined together using the equation shown below, the AUC could be further increased to 0.94

$$0.3 + 0.8 \times \text{Circularity} + 0.7 \times \text{Convexity}^{1/2} - 0.2 \times \text{Irregularity}^{1/2} - 0.1 \times \text{Compactness}^{1/2}. \quad (1)$$

A threshold value can be set to classify cases as either Type I or Type C, for example, a value less than 0.5 could represent Type I, while a value greater than 0.5 could represent Type C. The ROC curves can be generated using different threshold values, shown in Fig. 9. The results demonstrate that adding the other three parameters to the compactness index can further improve the AUC; therefore, they have a complementary role.

IV. DISCUSSION

In this work we developed an analysis method using quantitative morphological features to characterize the 3D distribution patterns of fibroglandular tissue. As an initial approach for validating the value of these quantitative morphological parameters, we investigated whether these param-

eters could differentiate between two distinct patterns (intermingled and central pattern) that could be easily separated visually. After excluding the 71 fatty breast cases with percent density $<7\%$, there were a total of 230 remaining cases. The ground truth to separate them into Type I and Type C was carefully established. The densities (percentage and volume) in these two groups were similar, and the ages of the patients in these two groups were also well matched. All four analyzed morphological features showed significant differences between these two patterns, and when combined they could achieve an AUC of 0.94 in the ROC analysis. The intermingled pattern had significantly higher compactness and irregularity and lower circularity and convexity indices compared to those of the central pattern. The results strongly suggest that it is feasible to characterize different distribution patterns of fibroglandular tissues using quantitative morphological measures.

We further explored the association of the extracted quantitative features with the visual MRI representation of fibroglandular tissue distribution. Examples from cases with high vs low index are demonstrated graphically in Figs. 5–8. The circularity and convexity indices were related to "shape," while irregularity index was more sensitive to "margin." The compactness index reflected the ratio between the surface area and the volume, and was associated with both shape and margin. Possibly due to its sensitivity to both shape and margin, the compactness had the greatest ability to differentiate between the intermingled and the central patterns. These results demonstrated that it is feasible to use quantitative parameters to describe the 3D density distribution on breast MRI.

Texture parameters are commonly used to analyze the density distribution on mammography. The analyzed texture information represents the amount and/or the heterogeneity/homogeneity of dense tissue distribution on mammograms. Because the texture parameters are analyzed on the projection image, one main contributing factor comes from the overlapping pattern of the dense and fatty tissues. For example, "skewness" can distinguish fatty tissues (positive value) from dense tissues (negative value).[18–20] Amadasun *et al.*[21] and Tahoces *et al.*[22] introduced another two texture features, coarseness and contrast, to describe the spatial relationship between fatty and dense tissues. There was evidence suggesting that the distribution of fibroglandular tissue is associated with cancer risk. Huo *et al.*[14] and Li *et al.*[1] used texture features to compare between the high-risk BRCA1/BRCA2 mutation carriers and low-risk women, and found that the BRCA1/BRCA2 mutation carriers tend to have more heterogeneously dense tissues (high coarseness and low contrast). Very recently, Manduca *et al.*[15] reported a systematic study to assess breast tissue texture using Markovian co-occurrence matrices, run-length analysis, Laws features, wavelet decomposition, and Fourier analysis. Following a comprehensive evaluation of a large community-based screening population of approximately 750 women, they have reported that the analyzed texture features predicted breast cancer risk at the same magnitude as did the percent breast density. The texture features at low spatial frequencies (i.e., coarser mammographic textures) were found to be the strongest predictors of breast cancer risk. However, the authors also commented that numerical values of texture features tend to vary with differences in acquisition variables such as compression force, angle, kVp, etc.

We would like to point out that the density analyzed based on mammogram cannot be generalized to predict the results analyzed from MRI. The density measurements by MRI and mammography have been shown highly correlated (Khazen *et al.*[23] $r=0.78$ for 138 high-risk women, Wei *et al.*[24] $r=0.89$ for 65 patients, Klifa *et al.*[25] $r=0.75$ for 15 cases, and Graham *et al.*[26] $r=0.79$ for 42 cases). However, all these studies also consistently showed that the mammographic density was higher than the density measured on MRI, which was attributed to two-dimensional vs three-dimensional image acquisitions. Mammography only acquires one projection image, and is not sufficient for analyzing the relative spatial distribution of dense and fatty tissues. On the other hand, MRI provides detailed 3D distribution patterns of fibroglandular tissue, hence not subject to the issue of tissue overlapping. Therefore, although both modalities show contrast between dense and fatty tissues, the texture results analyzed from mammography cannot be directly compared to the parenchymal patterns analyzed from dense tissue morphology on MRI. In fact, we have also performed texture analysis using gray level co-occurrence matrix and Laws texture features on MR images, but found them inferior to the morphology analysis reported here to differentiae between Type I and Type C.[27] In texture analysis, the entire image is analyzed, and a major part of the measured texture parameters is derived from the amount of fatty issue contained within the image, which is not of our interest. The morphology analysis approach used in this study is based on segmented fibroglandular tissue, and we believe that this provides much more specific information when compared to blind texture analysis.

It has been reported that the distribution of the mammary gland is associated with the development breast cancer.[12] For example, the BRCA1 and BRCA2 genes promote lobular branching, and the resulting denser and more heterogeneous breast parenchyma leads to increased cancer risk.[14] The risk for breast cancer associated with mammographic density may be explained by the combined effects of mitogens (which influence cell proliferation and the size of the cell population in the breast) and mutagens (which influence the likelihood of genetic damage to those cells).[28] Fatty tissue has been demonstrated to have the ability to generate products to augment the growth of mammary carcinoma cells.[13] Having more surface interaction between the fibroglandular and fatty tissue may be related to increased breast cancer risk by releasing lipid-soluble carcinogens into the intimate fibroglandular tissue. It is reasonable to expect that the intermingled pattern shown on MRI is more likely to show a heterogeneous pattern on 2D mammograms. Similar as the concept of using texture analysis on mammogram to correlate with risk, the MRI-based analysis technique that we reported in this work has the potential to facilitate the investigation of the relationship between breast parenchymal

pattern and cancer risk. We have provided strong evidence to demonstrate that the four analyzed parameters can differentiate between the central pattern and the intermingled pattern. To the best of our knowledge, no other group has ever reported on the analysis of breast density morphology based on MRI.

There are several limitations in this study. First, the data sets were from a research MRI database, therefore, it is not representing a general population. However, our purpose is to develop quantitative measures to distinguish between these two patterns (Type I and Type C), and as long as we have a good case number for each group, the data set can be used to test how well the quantitative parameters analyzed in this study can differentiate between these two groups. Second, we did not analyze the fatty breast cases. As shown in Fig. 1, since the contrast between fibroglandular and fatty tissues is not strong, the segmentation of the fibroglandular tissue may not be reliable for performing further morphology analysis. On the other hand, the fatty breasts can be easily classified based on the percent density alone, so further morphology analysis may not be needed. Third, the ground truth was established using visual inspection, which is subject to variations of observers. To minimize this observer bias, we had a total of three reading sessions by two observers (a radiologist and a physicist), and any case that had discrepant assignments among three readings was discussed to reach a consensus. Lastly, the best classifier combining all four morphological parameters was obtained using fourfold cross-validation within the same data set, not from independent training and validation data sets. To reduce variability, multiple rounds of cross-validation were performed using different partitions, and the validation results were averaged over the rounds. If an independent data set is available, we can further test the ability of each individual parameter and the combined classifier shown in Eq. (1) to differentiate between Type I and Type C patterns.

In summary, we have demonstrated that the four morphological parameters (circularity, convexity, irregularity, and compactness) can be used to characterize dense tissue distribution patterns based on MRI, and they can be used to investigate the relationship between parenchymal pattern and the cancer risk. For example, between two women who have similar percent density but have differing parenchymal patterns (e.g., central type vs mixed type), who will have a higher risk of developing cancer? Our method to characterize the morphology of the fibroglandular tissues provides an essential foundation for such research in the future. Breast density is a well-established risk factor, and a consensus has been reached by the Breast Cancer Prevention Collaborative Group to incorporate quantitative breast density into risk models.[29,30] The change in breast density has also been shown to be a good surrogate marker for predicting the efficacy of chemoprevention drugs.[31,32] In the future when the role of the morphological breast density features is established, they may also be incorporated into the risk models to further improve the accuracy in predicting each individual woman's cancer risk, for making an decision about the optimal management plan.

ACKNOWLEDGMENTS

This work was supported in part by NIH/NCI Grant Nos. R01 CA90437, R01 CA127927, R21 CA121568, and R03 CA136071, and California BCRP Grant Nos. 9WB-0020 and 14GB-0148.

[a]Author to whom correspondence should be addressed. Electronic mail: msu@uci.edu; Telephone: (949) 824-4925; Fax: (949) 824-3481.

[1]H. Li, M. L. Giger, O. I. Olopade, A. Margolis, L. Lan, and M. R. Chinander, "Computerized texture analysis of mammographic parenchymal patterns of digitized mammograms," Acad. Radiol. **12**, 863–873 (2005).
[2]J. Russo, H. Lynch, and I. H. Russo, "Mammary gland architecture as a determining factor in the susceptibility of the human breast to cancer," Breast J. **7**, 278–291 (2001).
[3]G. Ursin and M. Pike, "Mammographic density, hormone therapy, and risk of breast cancer," Cancer Epidemiol. Biomarkers Prev. **15**, 1750 (2006).
[4]N. F. Boyd, G. S. Dite, J. Stone, A. Gunasekara, D. R. English, M. R. E. McCredie, G. G. Giles, D. E. Tritchler, A. Chiarelli, M. J. Yaffe, and J. L. Hopper, "Heritability of mammographic density, a risk factor for breast cancer," N. Engl. J. Med. **347**, 886–894 (2002).
[5]N. F. Boyd, G. A. Lockwood, J. W. Byng, D. L. Tritchler, and M. J. Yaffe, "Mammographic densities and breast cancer risk," Cancer Epidemiol. Biomarkers Prev. **7**, 1133–1144 (1998).
[6]C. Byrne, C. Schairer, J. Wolfe, N. Parekh, M. Salane, L. A. Brinton, R. Hoover, and R. Haile, "Mammographic features and breast cancer risk: Effects with time, age, and menopause status," J. Natl. Cancer Inst. **87**, 1622–1629 (1995).
[7]C. Byrne, "Invited commentary: Assessing breast density change-lessons for future studies," Am. J. Epidemiol. **167**, 1037–1040 (2008).
[8]J. N. Wolfe, A. F. Saftlas, and M. Salane, "Mammographic parenchymal patterns and quantitative evaluation of mammographic densities: A case-control study," AJR, Am. J. Roentgenol. **148**, 1087–1092 (1987).
[9]G. Maskarinec, I. Pagano, G. Lurie, and L. N. Kolonel, "A longitudinal investigation of mammographic density: The multiethnic cohort," Cancer Epidemiol. Biomarkers Prev. **15**, 732–739 (2006).
[10]K. Kerlikowske, L. Ichikawa, D. L. Miglioretti, D. S. Buist, P. M. Vacek, R. Smith-Bindman, B. Yankaskas, P. A. Carney, and R. Ballard-Barbash, "Longitudinal measurement of clinical mammographic breast density to improve estimation of breast cancer risk," J. Natl. Cancer Inst. **99**, 386–395 (2007).
[11]C. M. Vachon, V. S. Pankratz, C. G. Scott, S. D. Maloney, K. Ghosh, K. R. Brandt, T. Milanese, M. J. Carston, and T. A. Sellers, "Longitudinal trends in mammographic percent density and breast cancer risk," Cancer Epidemiol. Biomarkers Prev. **16**, 921–928 (2007).
[12]A. E. Beer and R. E. Billingham, "Adipose tissue, a neglected factor in aetiology of breast cancer?," Lancet **312**, 296 (1978).
[13]J. E. Celis, J. M. Moreira, T. Cabezon, P. Gromov, E. Friis, F. Rank, and J. Gromova, "Identification of extracellular and intracellular signaling components of the mammary adipose tissue and its interstitial fluid in high risk breast cancer patients: Toward dissecting the molecular circuitry of epithelial-adipocyte stromal cell interactions," Mol. Cell. Proteomics **4**, 492–522 (2005).
[14]Z. Huo, M. L. Giger, O. I. Olopade, D. E. Wolverton, B. L. Weber, C. E. Metz, W. Zhong, and S. A. Cummings, "Computerized analysis of digitized mammograms of BRCA1 and BRCA2 gene mutation carriers," Radiology **225**, 519–526 (2002).
[15]A. Manduca, M. J. Carston, J. J. Heine, C. G. Scott, V. S. Pankratz, K. R. Brandt, T. A. Sellers, C. M. Vachon, and J. R. Cerhan, "Texture features from mammographic images and risk of breast cancer," Cancer Epidemiol. Biomarkers Prev. **18**, 837–845 (2009).
[16]K. Nie, J. H. Chen, S. Chan, M. K. Chau, H. J. Yu, S. Bahri, T. Tseng, O. Nalcioglu, and M. Y. Su, "Development of a quantitative method for analysis of breast density based on three-dimensional breast MRI," Med. Phys. **35**, 5253–5262 (2008).
[17]T. H. Cormen, C. E. Leiserson, L. R. Rivest, and C. Stein, *Introduction to Algorithm*, 2nd ed. (MIT Press, Cambridge, 2001).
[18]P. Taylor, S. Hajnal, M.-H. Dilhuydy, and B. Barreau, "Measuring image texture to separate 'difficult' from 'easy' mammograms," Br. J. Radiol. **67**, 456–463 (1994).

[19]J. W. Byng, M. J. Yaffe, G. A. Lockwood, L. E. Little, D. L. Tritchler, and N. F. Boyd, "Automated analysis of mammographic densities and breast carcinoma risk," Cancer **80**, 66–74 (1997).
[20]J. W. Byng, N. F. Boyd, E. Fishell, R. Jong, and M. J. Yaffe, "Automated analysis of mammographic densities," Phys. Med. Biol. **41**, 909–923 (1996).
[21]M. Amadasun and R. King, "Texture features corresponding to texture properties," IEEE Trans. Syst. Man Cybern. **19**, 1264–1274 (1989).
[22]P. G. Tahoces, J. Correa, M. Souto, L. Gómez, and J. J. Vidal, "Computer-aided diagnosis: The classification of mammographic breast parenchymal patterns," Phys. Med. Biol. **40**, 103–117 (1995).
[23]M. Khazen, R. M. Warren, C. R. Boggis, E. C. Bryant, S. Reed, I. Warsi, L. J. Pointon, G. E. Kwan-Lim, D. Thompson, R. Eeles, D. Easton, D. G. Evans, and M. O. Leach "A pilot study of compositional analysis of the breast and estimation of breast mammographic density using three-dimensional T1-weighted magnetic resonance imaging," Cancer Epidemiol. Biomarkers Prev. **17**, 2268–2274 (2008).
[24]J. Wei, H. P. Chan, M. A. Helvie, M. A. Roubidoux, B. Sahiner, C. Zhou, S. Paquerault, and M. M. Goodsitt, "Correlation between mammographic density and volumetric fibroglandular tissue estimated on breast MR images," Med. Phys. **31**, 933–942 (2004).
[25]C. Klifa, J. Carballido-Gamio, L. Wilmes, A. Laprie, C. Lobo, J. Gibbs, and N. Hylton, "Quantification of breast tissue index from MR data using fuzzy cluster," Conf. Proc. IEEE Eng. Med. Biol. Soc. **3**, 1667–1670 (2004).
[26]S. J. Graham, M. J. Bronskill, J. W. Byng, M. J. Yaffe, and N. F. Boyd, "Quantitative correlation of breast tissue parameters using magnetic resonance and x-ray mammography," Br. J. Cancer **73**, 162–168 (1996).
[27]K. Nie, J. H. Chen, S. Chan, O. Nalcioglu, and M. Y. Su, "Quantitative morphology and texture analysis of breast parenchymal pattern," Proceedings of the 16th ISMRM Annual Meeting, Toronto, Canada, 2008, p. 3763 (unpublished).
[28]L. J. Martin and N. F. Boyd, "Potential mechanisms of breast cancer risk associated with mammographic density: Hypotheses based on epidemiological evidence," Breast Cancer Res. **10**:201 (2008).
[29]C. E. Jacobi, G. H. de Bock, B. Siegerink, and C. J. Van Asperpen, "Differences and similarities in breast cancer risk assessment models in clinical practice: Which model to choose?," Breast Cancer Res. Treat. **115**, 381–390 (2009).
[30]R. J. Santen, N. F. Boyd, R. T. Chelbowski, S. Cummings, J. Cuzick, M. Dowsett, D. Easton, J. F. Forbes, T. Key, S. E. Hankinson, A. Howell, and J. Ingle, "Critical assessment of new risk factors for breast cancer: Considerations for development of an improved risk prediction model," Endocr. Relat. Cancer **14**, 169–187 (2007).
[31]J. Cuzick, J. Warwick, E. Pinney, L. R. M. Warren, and S. W. Duffy, "Change in breast density as a biomarker of breast cancer risk reduction; results from IBIS-1," Proceedings of the San Antonio Breast Cancer Symposium (SABCS), Abstract 61, 2008.
[32]J. Cuzick, J. Warwick, E. Pinney, R. M. Warren, and S. W. Duffy, "Tamoxifen and breast and breast density in women at increased risk of breast cancer," J. Natl. Cancer Inst. **21**, 621–628 (2004).